INORGANIC CHEMISTRY
FRONTIERS

RESEARCH ARTICLE

View Article Online
View Journal | View Issue

Cite this: *Inorg. Chem. Front.*, 2025, **12**, 7556

Accessing phosphonioacetylide chemistry: isolable alkali metal precursors for rod-shaped carbon donor complexes

Franka Brylak, [a] Pawel Löwe, [b] Klaus Wurst,[a] Stephan Hohloch [a] and Fabian Dielmann *[a]

Received 10th June 2025,
Accepted 23rd July 2025

DOI: 10.1039/d5qi01286d

rsc.li/frontiers-inorganic

Rod-shaped neutral carbon ligands such as carbon monoxide and isocyanides play a central role in organometallic chemistry but are relatively weak electron donors compared to N-heterocyclic carbenes. Phosphonioacetylides (R_3PCC) have been proposed as promising candidates for stronger electron donation within the class of sp-hybridized carbon ligands. However, their high reactivity has significantly limited their exploration and isolation. In this study, we report the synthesis and characterization of a novel phosphonioacetylide, MeR_2PCC (R = 1,3-di-*tert*-butylimidazolidin-2-ylidenamino). While it is highly labile at ambient temperature, the compound is stable at −40 °C and can be isolated and stored in the form of alkali metal complexes. The latter undergo efficient transmetallation reactions with a variety of electrophiles, enabling the formation of Lewis base adducts with both main group elements and transition metals, including tungsten(0), nickel(0), and rhodium(I). These results demonstrate that alkali metal phosphonioacetylides serve as versatile precursors for introducing this highly donating and structurally unique ligand into coordination complexes.

Introduction

Scientific advances in the field of coordination chemistry, material science and catalysis in recent decades have been driven by the development of neutral carbon ligands. New impetus has come especially from the development of N-heterocyclic carbenes (NHCs), which possess superior σ-donor properties compared to classical N- and P-donor ligands.[1–8] In light of the success story of carbene ligands, it is somewhat surprising that sp-hybridized carbon donor ligands with comparable donor properties have remained relatively underexplored. Typical sp-hybridized ligands such as carbon monoxide and isocyanides[9–17] are key components in organometallic chemistry, yet they exhibit weaker σ-donor strength than their sp^2- or sp^3-hybridized counterparts.[18–20] In this context, phosphonioacetylides, featuring a linear C_2 moiety bound to a phosphonium center, represent a promising and conceptually intriguing extension of the family of neutral, rod-shaped carbon ligands (Fig. 1). The modular nature of these species, particularly through variation of substituents at the phosphorus center, offers the potential to fine-tune their donor strength and vary the ambiphilic character of the terminal carbon atom.

The first phosphonioacetylide complex (**A**) was reported in 1970, synthesized *via* deoxygenation of a carbonyl ligand in $[Mn(CO)_5Br]$ using carbodiphosphorane Ph_3PCPPh_3 (Fig. 2).[21,22] In the following years, various phosphonioacetylide complexes were prepared through ligand transformations at metal centers.[23–36] Seeking a more general and direct route to such ligands, Bestmann and co-workers attempted the synthesis of a free phosphonioacetylide in 1998. They generated triphenylphosphonioacetylide (Ph_3PCC) by desilylation of the

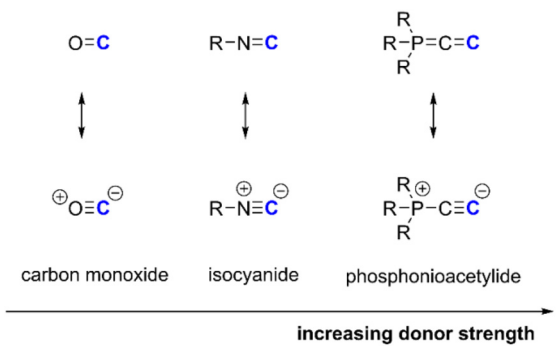

Fig. 1 Selection of sp-hybridized neutral carbon ligands and their resonance structures.

[a]*Institute of General, Inorganic and Theoretical Chemistry, Universität Innsbruck, Innrain 80-82, 6020 Innsbruck, Austria. E-mail: fabian.dielmann@uibk.ac.at*
[b]*Institute for Inorganic and Analytical Chemistry, Universität Münster, 48149 Münster, Germany*

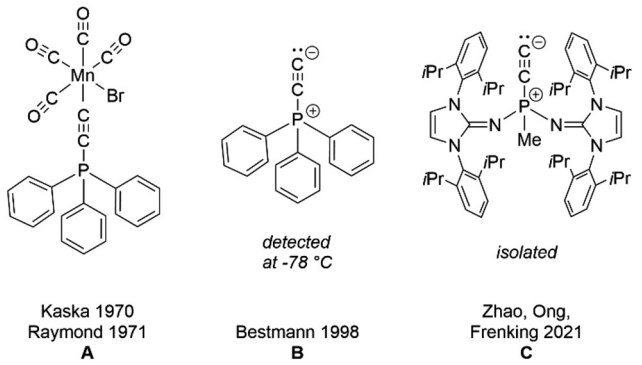

Fig. 2 Milestones of phosphonioacetylides: the first phosphonioacetylide complex **A** (left), the first free phosphonioacetylide identified spectroscopically at −78 °C (**B**, middle), the first room-temperature stable free phosphonioacetylide **C** (right).

cationic precursor $[Ph_3PCCSiMe_3]^+$ with a fluoride source at −78 °C and characterized the fleeting intermediate by NMR spectroscopy (Fig. 2), which could not be isolated because it proved to decompose rapidly at ambient temperature.[37,38] In 2009, Hill and co-workers seized on this work and investigated the reactivity and ligand properties of Ph_3PCC (**B**). The comparison of the frontier molecular orbital energies indicate that Ph_3PCC has similar π-acceptor properties but is a significantly better σ- and π-donor than methyl isocyanide.[39] The first room temperature stable phosphonioacetylide (**C**) was reported in 2021 by Zhao, Ong, and Frenking (Fig. 2). Electron-donating bulky N-heterocyclic imine (NHI) substituents bearing 2,6-diisopropylphenylgroups (dipp) at the nitrogen atoms of the heterocycle were used to stabilize the reactive PC_2 unit.[40]

As part of our ongoing efforts to develop electron-rich ligands, including phosphines,[41–45] pyridines,[46,47] and porphyrins,[48] we utilized the π-donating power and tunability of NHI substituents[49–52] to enhance their electron-donating capabilities. Recently, our focus shifted towards stabilizing neutral carbon ligands, such as carbenes and cumulenes.[53–56] In this study, we report on our efforts to expand the class of isolable phosphonioacetylides, as the structural factors governing their stability remain poorly understood. Addressing these knowledge gaps could unlock broader applications of phosphonioacetylides in coordination chemistry and catalysis. To this end, we investigated how introducing small NHI substituents at the phosphonium center influences the stability and ligand properties of phosphonioacetylides.

Results and discussion

In analogy to the previously reported synthetic route,[40] ethynyl phosphine **1** was synthesized using HCCMgCl for alkynylation of our previously reported phosphenium ion, bearing *tert*-butyl groups at the N-heterocyclic nitrogens of the NHI substituents.[57,58] Subsequent methylation with either methyl iodide or methyl triflate afforded the phosphonium salts [**2**]X (X = I, OTf) in good yields. Attempts to deprotonate [**2**]X using various inorganic bases, including *n*BuLi, potassium *tert*-butoxide (KO*t*Bu), potassium hexamethyldisilazide (KHMDS) or neutral bases including the phosphonium ylide Ph_3PCH_2 and the superbasic phosphine $P(tmg)_3$,[59] generally led to unselective decomposition upon warming to ambient temperature, as indicated by the presence of multiple phosphorus-containing species observed by ^{31}P NMR spectroscopy (see the SI). One notable decomposition pathway appeared to involve cleavage of the C_2 unit, as evidenced by resonance at 69.1 ppm corresponding to phosphine $MePR_2$.[54] Through extensive screening of different base/phosphonium salt combinations, we found that the well-defined lithium complex $[R_2MePCCLi(thf)_2I]$ (**3**) and the labile potassium complex $[R_2MePCCKOTf]$ (**4**) are both isolable and remain stable at ambient temperature when stored under an inert atmosphere.

Treatment of [**2**]I with *n*BuLi in THF at −40 °C, followed by immediate evaporation of the volatiles, afforded the lithium complex **3** as a white solid in very good yield (Fig. 3). Compound **3** is soluble in both polar and nonpolar solvents, including THF and toluene. However, **3** decomposes in chloroform, DCM and ACN. Successful deprotonation is confirmed by the disappearance of the alkynyl proton resonance in the ^1H NMR spectrum and the appearance of a quartet at −41.0 ppm ($^2J_{PH}$ = 14 Hz) in the ^{31}P NMR spectrum. In the $^{13}C\{^1H\}$ NMR spectrum, the α and β alkynyl carbon atoms of **3** exhibit significant shifts to higher frequency compared to the phosphonium precursor $[\mathbf{2}]^+$ (**3**: 106.1 ppm (C_α), 170.6 ppm (C_β); $[\mathbf{2}]^+$: 81.3 ppm (C_α), 91.9 ppm (C_β)). In contrast, the terminal carbon atoms in free phosphonioacetylides **B** (228.9 ppm)[37,38] and **C** (208.5 ppm in THF-d_8, 218.1 ppm in C_6D_6)[40] resonate at even higher frequency, suggesting lithium coordination in **3**. Notably, similar trends have been observed for lithium complexes of other carbon nucleophiles, such as Bertrand's cyclopropenylidene and allenylidene.[60,61] Further evidence for the formation of a lithium-stabilized phosphonioacetylide complex is provided by the detection of a distinct $^7Li\{^1H\}$ NMR signal at 1.4 ppm. The ^1H NMR spectrum also indicates coordination of the lithium cation by two additional THF molecules. Single-crystal X-ray diffraction (SCXRD) analysis revealed that **3** adopts a dimeric structure in the solid state (Fig. 3d). Each lithium cation is tetrahedrally coordinated by two THF molecules and two bridging phosphonioacetylide ligands, resulting in a four-membered Li_2C_2 ring with iodide as counterion. The C1–C2 bond length of 1.220(2) Å is consistent with a typical triple bond (1.21 Å; *cf.* double bond: 1.33 Å),[62] the P1–C2 bond length with 1.742(14) Å is between typical phosphorus carbon single and double bonds (single bond: 1.87 Å, double bond: 1.67 Å)[63] and the P–C–C bond angle approaches linearity at 176.5(13)°.

A second viable synthetic route to an isolable phosphonioacetylide alkali metal complex was identified *via* deprotonation of the triflate salt [**2**]OTf using a slight excess of KHMDS. Treatment of [**2**]OTf with KHMDS in THF afforded the phosphonioacetylide complex **4**, which was isolated as a white solid in 67% yield after workup. The potassium complex

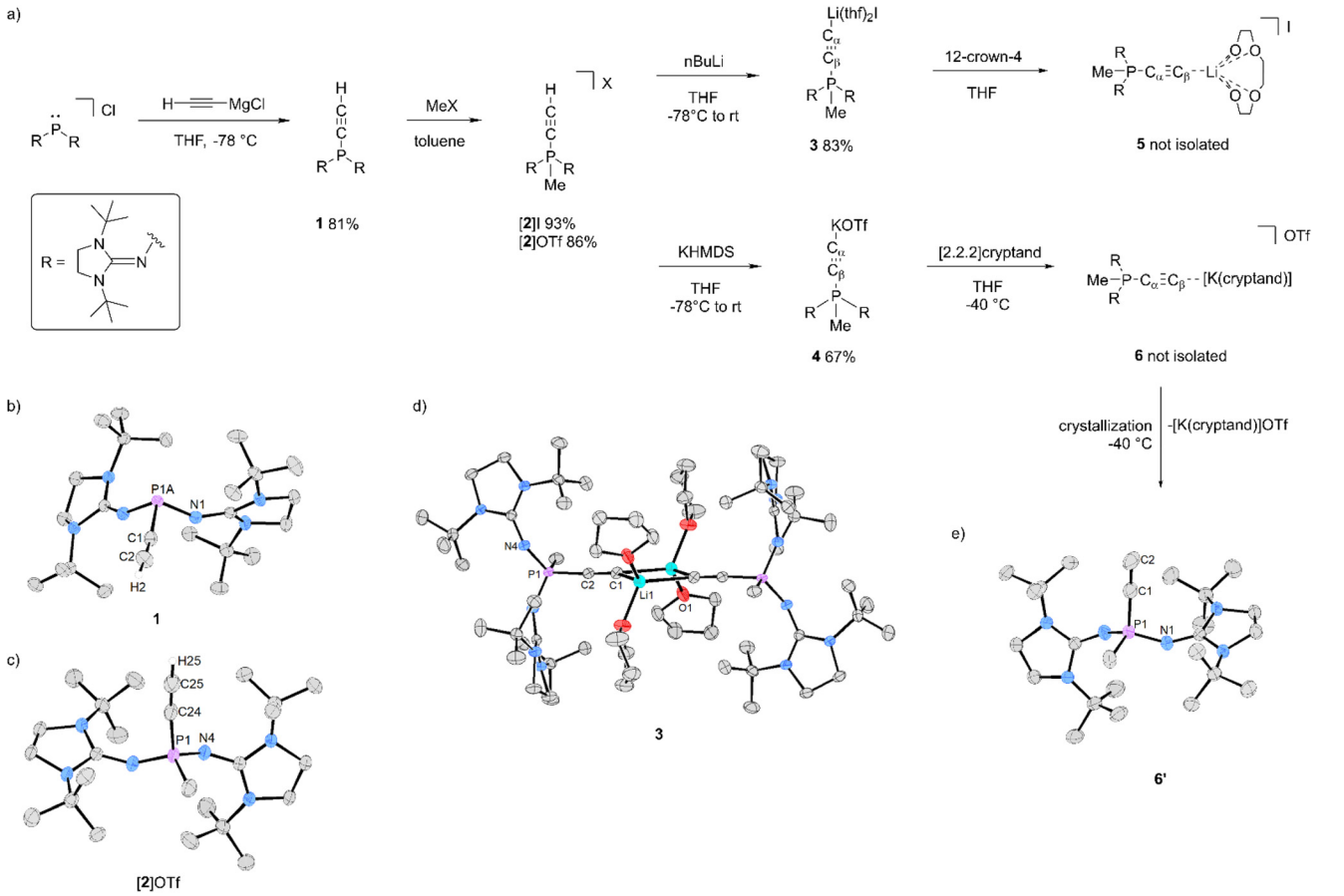

Fig. 3 (a) Synthesis of the alkali metal phosphonioacetylide complexes **3**–**6**. Solid-state structures of (b) **1**, (c) [**2**]OTf, (d) **3** and (e) **6′**. Hydrogen atoms except the hydrogen attached at C_β and counter ions (triflate for [**2**]OTf, iodide for **3**) are omitted for clarity. Ellipsoids are displayed at 50% probability. Selected structural data is shown in Table 1.

exhibits good solubility in THF, toluene and benzene, and its spectroscopic features are consistent with the presence of the PC_2 moiety. Notably, the ^{31}P NMR spectrum displays a signal at −43.8 ppm (quartet, $^2J_{PH}$ = 14 Hz), while the ^{13}C NMR spectrum shows a resonance at 105.2 ppm corresponding to C_α, closely resembling the data obtained for the lithium complex **3**. The ^{13}C NMR signal for the terminal carbon atom (C_β) was observed at 201.0 ppm in deuterated THF. Compared with the lithium complex **3** (170.6 ppm), this resonance is significantly shifted to higher frequency suggesting a much weaker carbon-potassium interaction. Compound **4** can be stored as a solid under an inert atmosphere. Notably, the isolated material consistently retained sub-stoichiometric amounts of Et_2O, THF and HMDS, which could not be completely removed even after extended drying under reduced pressure. Consequently, compound **4** was typically generated *in situ* for subsequent ligand transfer reactions (*vide infra*).

Liberation of the free phosphonioacetylide was attempted *via* sequestration of the lithium and potassium metal ions using 12-crown-4 and [2.2.2]cryptand, respectively. Treatment of **3** with stoichiometric amounts of 12-crown-4 resulted in the formation of the lithium complex **5**. The analysis of the NMR data reveals a shift in the ^{13}C resonance of the terminal β carbon to 183.5 ppm, suggesting a weakening of the coordinative bond. Furthermore, a significant shift to lower frequency in the ^7Li NMR to −0.3 ppm is observed, consistent with the replacement of THF by 12-crown-4 in the lithium coordination sphere.[64] Complex **5** proved to be highly labile, as the removal of solvent followed by redissolution led to partial decomposition. Moreover, the addition of more than one equivalent of 12-crown-4 resulted in the complete decomposition of the phosphonioacetylide. This behaviour suggests successful cleavage of the lithium-carbon bond, as lithium ions are known to coordinate with two crown ether molecules.[65] Similarly, the addition of stoichiometric amounts of [2.2.2] cryptand to a THF solution of complex **4** caused the ^{13}C resonance of the β carbon to shift to higher frequency (215.6 ppm). This chemical shift falls within the range observed for **B** (228.9 ppm) and **C** (208.5 ppm), suggesting that the liberation of the phosphonioacetylide was either successful or that the C terminus remains weakly coordinated to the potassium ion within the cryptand cage. The latter possibility aligns with previous observations by Rosokha and coworkers for other rod-shaped ligands.[66] Supporting this interpretation, attempts to

separate the free phosphonioacetylide by benzene extraction were unsuccessful. However, when the reaction mixture was stored at −40 °C, two distinct types of crystals formed: colorless blocks and brown needles. Structural analysis *via* SCXRD identified these as the salt [K(cryptand)]OTf and the free phosphonioacetylide **6′**, respectively (Fig. 3e). Notably, the C1–C2 bond length of **6′** (1.203(5) Å) is slightly shorter than in complex **3**, while the P1–C1 bond length is elongated to 1.765 (2) Å.

Collectively, the deprotonation and sequestration experiments demonstrate that the generation of the phosphonioacetylide requires stabilization through the formation of alkali metal complexes, which prevent decomposition *via* reaction with the phosphonium precursor. Furthermore, the liberation of the phosphonioacetylide by sequestration of the alkali metals is achievable. While the free ligand is stable at low temperatures, it appears to be transient and unstable at room temperature.

Next, the hydrolytic stability of **3** was investigated. Treatment of **3** in THF with ten equivalents H_2O quantitively yielded the precipitation of the protonated alkynyl salt [**2**]I, which already suggests that the free phosphonioacetylide is highly basic, as lithium hydroxide is generated in the reaction.

Treatment of **3** with the Lewis acid $B(C_6F_5)_3$ led to the corresponding borane adduct **7**, which was isolated as a white solid in 50% yield. The carbon signal of C_β in the ^{13}C NMR spectrum (123.0 ppm) is shifted to lower frequency by 47.6 ppm compared to that of **3**. In addition, the boron resonance at −21.5 ppm in the $^{11}B\{^1H\}$ NMR spectrum confirms the formation of a borate species, as this chemical shift is significantly shifted to lower frequency compared to free $B(C_6F_5)_3$ (60 ppm).[67] Further evidence for the adduct formation comes from the $^{31}P\{^1H\}$ NMR spectrum, which shows distinct boron-phosphorus coupling, observed as a doublet with a coupling constant of $^3J_{BP}$ = 4 Hz. These spectroscopic features are consistent with alkynylphosphonium borates previously reported by Bestmann, Stephan and Erker.[32,33,37,38,68,69] Notably, the ^7Li NMR spectrum of the isolated solid of **3** indicated the presence of trace amounts of lithium iodide, even after extraction and recrystallization, although an SCXRD study confirmed the successful separation (*vide infra*). This observation indicates a limitation of using **3** in transmetallation reactions, as the nitrogen atoms of the NHI groups can act as chelating ligands for lithium salts, thereby making the separation more difficult. Moreover, an additional potentially undesired reaction pathway was observed when **3** was treated with $[Rh(cod)Cl]_2$. This reaction produced a mixture of rhodium complexes [Rh(CCPMeR$_2$)(cod)Cl] (**11**) and [Rh(CCPMeR$_2$)(cod)I] (**11′**) due to anion scrambling (Fig. S73). Anion scrambling, particularly with halogens, is a well-documented issue.[70,71] It is typically mitigated by avoiding reactants with different halogens or by replacing chloride in $[Rh(cod)Cl]_2$ with silver triflate in the presence of coordinating solvents such as acetonitrile or THF. However, anion scrambling between halogens and triflates is uncommon due to the much weaker coordination properties of the latter. Therefore, we used the triflate complex **4** in subsequent transmetallation studies, which was generated *in situ via* deprotonation of [**2**]OTf with suitable potassium bases.

The reaction with TMSCl and the transition metal complexes $[W(CO)_5(thf)]$ and $[Rh(cod)Cl]_2$ resulted in complete conversion to the corresponding terminal phosphonioacetylide complexes **8**, **9** and **11** (Fig. 4a, right). These complexes were isolated in moderate yield after workup and separation of the potassium salts. In contrast, the reaction with $[Ni(CO)_4]$ led to the formation of a side product, which complicated the separation process and thus gave **10** in low yield. ^{31}P NMR spectra of the phosphonioacetylide complexes show resonances as quartets with coupling constants of $^2J_{PH}$ = 14–15 Hz, and their chemical shifts fall within a very similar range (Table 1). For complex **11**, an additional coupling constant of $^3J_{PRh}$ = 4 Hz was observed, consistent with the terminal coordination of the C_2 unit in this complex. An overview of the ^{13}C NMR resonances for the acetylide units in the phosphonioacetylide complexes is provided in Table 1. The C_α and C_β signals were assigned based on their distinct coupling constant to the phosphorus nucleus. These signals follow a trend of shifting to lower frequency as the covalency of the carbon–element bond increases, whereas they appear at higher frequency for more ionic carbon–element bonds.

SCXRD studies of complexes **7**, **9**, **10** and **11′** confirmed the formation of terminal phosphonioacetylide complexes (Fig. 4). Selected structural parameters are summarized in Table 1. The observed C≡C and the P–C bond lengths are comparable to those in the lithium complex **3**. However, when compared to the phosphonium cation **2**, the C≡C bonds are elongated, and the P–C bonds are shortened. This suggests a significant allenylidene-type character of the PCC moiety due to π-backbonding from the anionic acetylide moiety into the σ* orbitals of the phosphonium unit. Further supporting the presence of allenylidene character, the PCC angles deviate more significantly from linearity than the CCE bond angles. This systematic deviation is thus unlikely to arise from crystal packing effects.

With complex **10** in hand, the donor strength of the new phosphonioacetylide ligand was determined using the Tolman electronic parameter (TEP)[72] The symmetric A_1 carbonyl stretching frequency of complex **10** was experimentally observed in DCM at 2050.1 cm^{-1}. Notably, a significantly lower TEP value of 2023 cm^{-1} was reported for phosphonioacetylide **C**, which, however, was converted from the corresponding rhodium complex $[Rh(CO)_2Cl(\mathbf{C})]$.[73] To investigate this discrepancy, DFT calculations were performed to compute the TEP values for both phosphonioacetylides, following the method reported by Gusev.[74] The calculated TEP derived from complex **10** (2055.0 cm^{-1}) and from $[Ni(CO)_3\mathbf{C}]$ (2051.1 cm^{-1}) are in close agreement with the experimentally observed A_1 stretching frequency of **10**, highlighting the new phosphonioacetylide ligand as a strong donor with an overall donor ability comparable to that of classical N-heterocyclic carbenes.[75,76] Additionally, for $[Ni(CO)_3\mathbf{B}]$, a TEP value of 2068.3 cm^{-1} was calculated, demonstrating a significant impact of NHI group substitution at the phosphonium on the ligand's donor

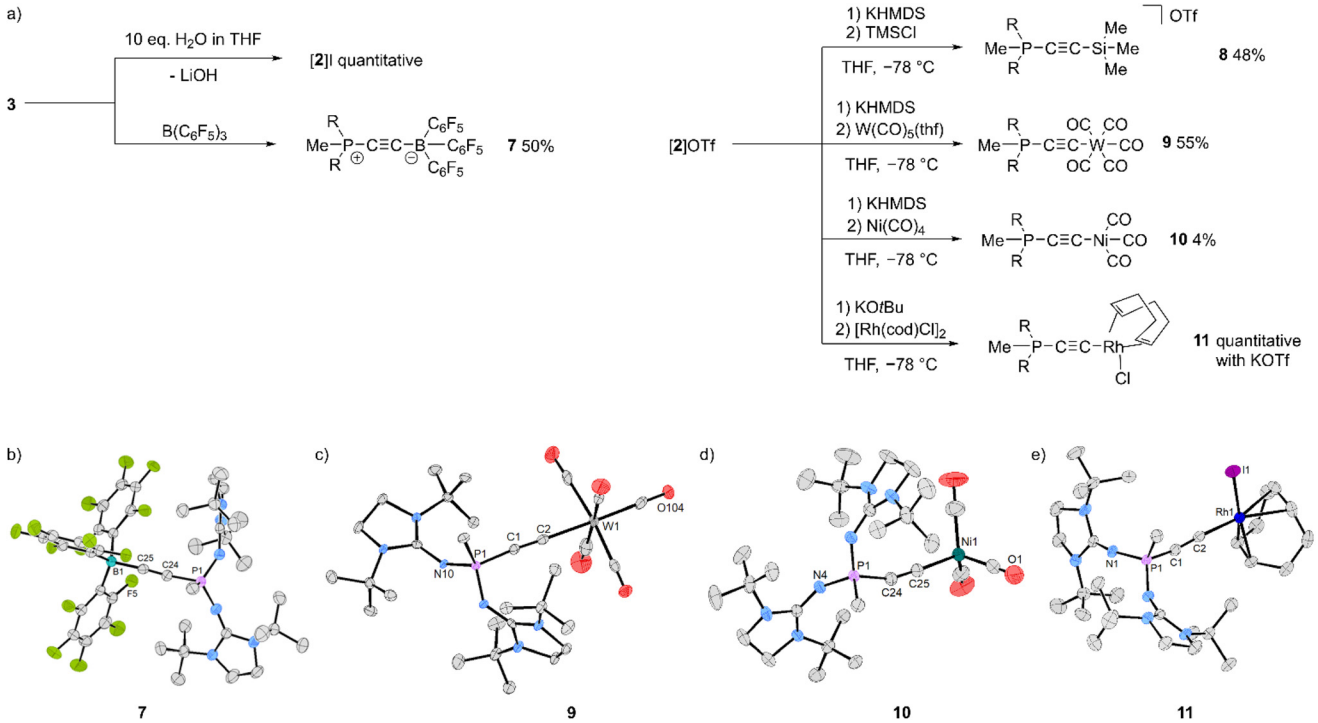

Fig. 4 (a) Transmetallation reactions using either the lithium salt **3** or the potassium salt **4**. The latter was generated *in situ* by deprotonation of [**2**]OTf with KHMDS or KO*t*Bu. Solid-state structures of (b) **7**, (c) **9**, (d) **10** and (e) **11′**. Hydrogen atoms and solvent molecules are omitted for clarity. Ellipsoids are displayed at 50% probability. Selected structural data is shown in Table 1. R = di-*tert*-butylimidazolidin-2-ylidenamino.

Table 1 Selected solution NMR data and structural parameters of the solid-state structures of compounds **1–10**

Compound	^{31}P NMR shift in ppm	^{13}C NMR shift of C_α in ppm	^{13}C NMR shift of C_β in ppm	C≡C bond length in Å	P–C bond length in Å	P–C–C bond angle in °	C–C–E bond angle in °	% V_{bur} [f]
1	53.2 (s)[a]	93.3 (d, $^1J_{CP}$ = 46 Hz)[a]	85.4 (d, $^2J_{CP}$ = 5 Hz)[a]	1.180(3)	1.8138(19)	170.35(19)	—	—
2	−41.7 (p, J_{PH} = 15 Hz)[b]	81.4 (d, $^1J_{CP}$ = 190 Hz)[b]	91.9 (d, $^2J_{CP}$ = 34 Hz)[b]	1.185(3)	1.769(2)	174.4(2)	—	—
3	−41.0 (q, $^2J_{PH}$ = 14 Hz)[a]	106.1 (d, $^1J_{CP}$ = 164 Hz)[a]	170.6 (br)[a]	1.220(2)	1.7417(14)	176.52(13)	136.06(14) (X = Li1), 151.85(15) (X = Li1′)	18.6
4	−43.9 (q, $^2J_{PH}$ = 14 Hz)[a]	104.3 (d, $^1J_{CP}$ = 159 Hz)[d]	201.0 (d, $^2J_{CP}$ = 9 Hz)[d]	—	—	—	—	—
5	−42.9 (q, $^2J_{PH}$ = 14 Hz)[a]	101.8 (d, $^1J_{CP}$ = 170 Hz)[a]	183.5 (br)[a]	—	—	—	—	—
6	−48.8 (q, $^2J_{PH}$ = 14 Hz)[d]	103.7 (d, $^1J_{CP}$ = 155 Hz)[d]	215.6 (d, $^2J_{CP}$ = 15 Hz)[d]	—	—	—	—	—
6′	—	—	—	1.203(5)	1.765(2)	174.0(3)	—	18.9
7	−39.6 (m)[c]/−39.6 (d, $^3J_{BP}$ = 4 Hz)[c,e]	90.0 (d, $^1J_{CP}$ = 197 Hz)[c]	123.0 (br)[c]	1.206(3)	1.7437(18)	168.02(17)	175.44(19)	18.2
8	−41.4 (q, $^2J_{PH}$ = 15 Hz)[b]	102.2 (d, $^1J_{CP}$ = 175 Hz)[b]	111.1 (d, $^2J_{CP}$ = 23 Hz)[b]	—	—	—	—	—
9	−42.3 (q, $^2J_{PH}$ = 14 Hz)[a]	104.9 (d, $^1J_{CP}$ = 197 Hz)[a]	151.7 (d, $^2J_{CP}$ = 20 Hz)[a]	1.214(4)	1.727(3)	175.5(3)	178.0(3)	19.8
10	−41.5 (q, $^2J_{PH}$ = 15 Hz)[a]	104.6 (d, $^1J_{CP}$ = 193 Hz)[a]	170.5 (d, $^2J_{CP}$ = 15 Hz)[a]	1.220(2)	1.7300(15)	160.66(14)	176.07(14)	20.5
11/11′	−40.7 (qd, $^2J_{PH}$ = 14 Hz, $^3J_{PRh}$ = 4 Hz)[a]	—	—	1.2196(18)	1.7314(13)	156.95(12)	175.78(11)	19.3

[a] Recorded in C_6D_6. [b] Recorded in CD_3CN. [c] Recorded in CD_2Cl_2. [d] Recorded in THF-d_8. [e] $^{31}P\{^1H\}$ NMR shift. [f] Bondi radii scaled by 1.17, sphere radius = 3.5, C_β selected to coordinate to centre of the sphere with distance of 2.0, mesh spacing for numerical integration = 0.1, H atoms not included.

properties. These findings are consistent with the well-established influence of substituents on phosphines, as described by Tolman's substituent parameter, χ_i.[77] The steric bulk of the new phosphonioacetylide ligand was evaluated by calculating the buried volume ($\%V_{bur}$)[78–80] based on the solid-state structures of the corresponding complexes (Table 1). Due to the rod-shaped structure of the ligand, the bulky NHI groups have minimal influence on the coordination sphere around the metal centre, confining the 3.5 Å sphere to a $\%V_{bur}$ value of 18.2–20.5%. This analysis indicates that the new phosphonioacetylide ligand exhibits steric properties comparable to those of triphenylphosphonioacetylide ($\%V_{bur}$ = 17.5 for complex [W(CCPPh$_3$)(CO)$_5$]),[36] but it is significantly less sterically demanding than phosphonioacetylide **C** ($\%V_{bur}$ = 32.4 for complex $[Au(\mathbf{C})_2]^+$).[73]

The reactivity studies presented here highlight the high nucleophilicity and basicity of the new phosphonioacetylide **6′**, as well as its ability to function as a strong donor ligand. Like other common neutral C- and P-donor ligands, such as NHCs and phosphines, **6′** readily forms transition metal complexes. However, its unique rod-shaped structure allows it to form Lewis adducts even with bulky Lewis acids, such as tris(pentafluorophenyl)borane, which typically resist adduct formation with bulky phosphines or NHCs, often resulting in frustrated Lewis pair systems.[81–83]

Density functional theory calculations at the B3LYP/6-311G(d) level were carried out to gain an insight into the ligand properties of phosphonioacetylide **6′** and investigate how these are influenced by phosphorus substituents and interactions with alkali metal cations. As demonstrated by Wagler and coworkers, the frontier orbital energies relevant for σ-, π-donor and π-acceptor interactions reveal that common sp-hybridized ligands, such as carbon monoxide and isocyanides, are significantly weaker σ and π donors compared to phosphonioacetylide **B** (Fig. 5). The introduction of NHI substituents destabilizes both donor and acceptor orbitals by approximately 1 eV, leading to superior donor and weaker π-acceptor ability in the case of **6′**. This trend aligns with natural bond orbital (NBO) analysis, which shows that NHI substitution increases the negative charge on the C_2 unit by 0.11 eV, with the most pronounced increase at C_β (Table 2). Simultaneously, Wiberg bond indices indicate reduced backbonding from the C_2 unit to phosphorus. The phosphorus atom carries a large positive charge, which is further amplified by the electronegative nitrogen atoms of the NHI substituents. The charge distribution supports the resonance structure shown in Fig. 5, with the NHI substituents promoting increased donation of the C_α negative charge toward C_β. This is further corroborated by Wiberg bond indices, which show a higher C_α–C_β bond order for **6′** (2.59) compared to **B** (2.53). Notably, coordination to alkali metals significantly reduces the polarity of the C_2 unit by redistributing charge toward C_β and increasing the C_α–C_β bond order, while the overall negative charge of the C_2 unit increases only slightly. This effect is more pronounced with the strongly polarizing lithium cation. These results support experimental observations that **6′** is effectively stabilized by coordination to alkali metal ions, particularly lithium. Furthermore, they suggest that lithium complexes of other phosphonioacetylides, such as **B**, should also be isolable and stable under ambient conditions.

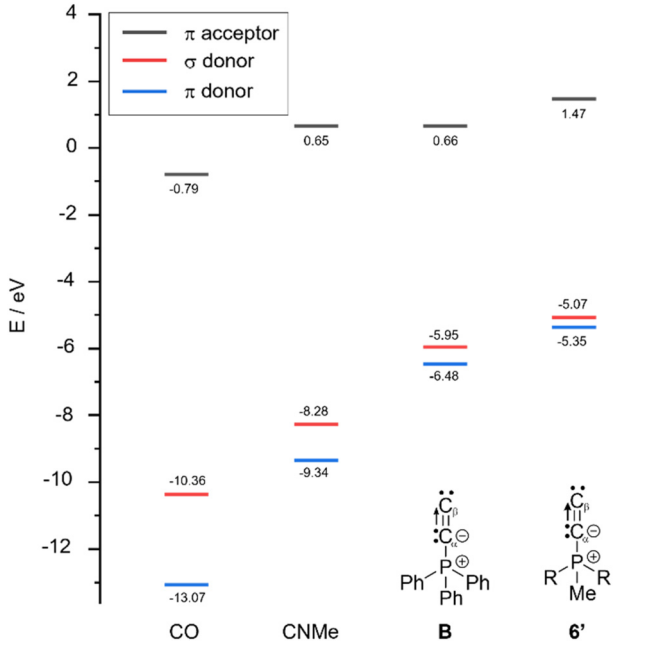

Fig. 5 Relative energies of the frontier orbital relevant for σ-, π-donor and π-acceptor interactions calculated with B3LYP/6-311G(d).

Table 2 Selected calculated natural atomic charges and Wiberg bond indices with B3LYP/6-311G(d). R = di-*tert*-butylimidazolidin-2-ylidenamino

Compound	P in *e*	C_α in *e*	C_β in *e*	Li/K in *e*	P–C_α	C_α–C_β	C_β–Li/K
$Ph_3PCC\text{-}Li^+$	1.57	−0.66	−0.42	0.95	1.01	2.80	0.09
$Ph_3PCC\text{-}K^+$	1.57	−0.76	−0.29	0.97	1.03	2.74	0.01
Ph_3PCC (**B**)	1.57	−0.97	0.00	—	1.11	2.53	—
$R_2MePCC\text{-}Li^+$	1.98	−0.65	−0.53	0.94	0.90	2.84	0.11
$R_2MePCC\text{-}K^+$	1.98	−0.75	−0.40	0.95	0.93	2.79	0.09
R_2MePCC (**6′**)	1.98	−0.98	−0.10	—	1.02	2.59	—

Experimental section

All experimental details are included in the SI.

Conclusions

In summary, a new rod-shaped phosphonioacetylide ligand is reported including its synthesis, properties, and coordination chemistry. By employing less bulky NHI groups at the phosphonium centre compared to the isolable phosphonioacetylide **C**, we successfully tuned the steric and electronic properties of this largely unexplored ligand class. Due to the better

accessibility of the reactive C_2 unit, the free ligand is highly labile at ambient temperature but sufficiently stable at −40 °C to allow its structural characterization. In contrast, the corresponding lithium and potassium complexes (**3** and **4**) can be stored at ambient temperature, making them suitable for further reactivity studies. These alkali metal complexes readily undergo transmetallation with various electrophiles, providing straightforward access to terminal phosphonioacetylide complexes.

The new ligand exhibits high basicity and nucleophilicity, clearly outperforming common sp-hybridized neutral carbon ligands such as carbon monoxide and isocyanides in terms of donor strength. Its donor ability is comparable to that of classical N-heterocyclic carbenes, while its low steric bulk enhances its versatility. With this unique combination of strong donor properties and minimal steric hindrance, the rod-shaped ligand is expected to be of significant interest in coordination chemistry, particularly in systems requiring multiple strong donor ligands.

Author contributions

Synthetic experimentation was performed by F. B. (**2**–**11**) and P. L. (**1**). The project was directed by F. D. Computations were performed by F. B. SCXRD studies were performed by P. L. (**1**), K. W. ([**2**]I, [**2**]OTf, **3**, **7**, **10**, **11**′) and S. H. (refinement of **9**). The manuscript was written and edited by F. B. and F. D. All authors have given approval for the final version of the manuscript.

Conflicts of interest

There are no conflicts to declare.

Data availability

The data supporting this article have been included as part of the SI.

Supplementary information including experimental and computational details is available See DOI: **https://doi.org/10.1039/d5qi01286d**.

CCDC 2456627–2456634 and 2472604 contain the supplementary crystallographic data for this paper.[84a–i]

Acknowledgements

F. B. gratefully acknowledges financial support by a doctoral scholarship of the Universität Innsbruck. P. L. acknowledges the support of the DFG (IRTG 2027). We thank Priv.-Doz. Dr Alexander Pöthig and the Catalysis Research Center at Technische Universität München for providing access to the XRD instrument for the SCXRD study of 9. We thank Lena Lezius for her help with DFT calculations and Dr Michael Seidl for editing of the SCXRD part of the SI and SCXRD studies of **6**′. The computational results presented here have been achieved in part using the LEO HPC infrastructure of the University of Innsbruck.

References

1 P. Bellotti, M. Koy, M. N. Hopkinson and F. Glorius, Recent advances in the chemistry and applications of N-heterocyclic carbenes, *Nat. Rev. Chem.*, 2021, **5**, 711–725.
2 D. Bourissou, O. Guerret, F. P. Gabbaï and G. Bertrand, Stable Carbenes, *Chem. Rev.*, 2000, **100**, 39–92.
3 H. Jacobsen, A. Correa, A. Poater, C. Costabile and L. Cavallo, Understanding the M(NHC) (NHC=N-heterocyclic carbene) bond, *Coord. Chem. Rev.*, 2009, **253**, 687–703.
4 M. N. Hopkinson, C. Richter, M. Schedler and F. Glorius, An overview of N-heterocyclic carbenes, *Nature*, 2014, **510**, 485–496.
5 W. A. Herrmann and C. Köcher, N-Heterocyclic Carbenes, *Angew. Chem., Int. Ed. Engl.*, 1997, **36**, 2162–2187.
6 W. A. Herrmann and C. Köcher, N–Heterocyclische Carbene, *Angew. Chem.*, 1997, **109**, 2256–2282.
7 W. A. Herrmann, N-Heterocyclic Carbenes: A New Concept in Organometallic Catalysis, *Angew. Chem., Int. Ed.*, 2002, **41**, 1290–1309.
8 W. A. Herrmann, N-Heterocyclische Carbene: ein neues Konzept in der metallorganischen Katalyse N-Heterocyclische Carbene, *Angew. Chem.*, 2002, **114**, 1342.
9 M. Knorn, E. Lutsker and O. Reiser, Isonitriles as supporting and non-innocent ligands in metal catalysis, *Chem. Soc. Rev.*, 2020, **49**, 7730–7752.
10 S. Wang, J. D. Sears, C. E. Moore, A. L. Rheingold, M. L. Neidig and J. S. Figueroa, Side-on coordination of diphosphorus to a mononuclear iron center, *Science*, 2022, **375**, 1393–1397.
11 L. A. Büldt, X. Guo, A. Prescimone and O. S. Wenger, A Molybdenum(0) Isocyanide Analogue of Ru(2,2′-Bipyridine)$_3^{2+}$: A Strong Reductant for Photoredox Catalysis, *Angew. Chem., Int. Ed.*, 2016, **55**, 11247–11250.
12 L. A. Büldt, X. Guo, A. Prescimone and O. S. Wenger, Ein Molybdän(0)–Isocyanid–Komplex als Ru(2,2′–Bipyridin)$_3^{2+}$–Analogon: ein starkes Reduktionsmittel für die Photoredoxkatalyse, *Angew. Chem.*, 2016, **128**, 11413–11417.
13 L. A. Büldt, X. Guo, R. Vogel, A. Prescimone and O. S. Wenger, A Tris(diisocyanide)chromium(0) Complex Is a Luminescent Analog of Fe(2,2′-Bipyridine)$_3^{2+}$, *J. Am. Chem. Soc.*, 2017, **139**, 985–992.
14 L. A. Büldt and O. S. Wenger, Chromium(0), Molybdenum (0), and Tungsten(0) Isocyanide Complexes as Luminophores and Photosensitizers with Long-Lived Excited States, *Angew. Chem., Int. Ed.*, 2017, **56**, 5676–5682.
15 L. A. Büldt and O. S. Wenger, Isocyanid–Komplexe von Cr^0, Mo^0 und W^0 als Leuchtstoffe und Photosensibilisatoren mit langlebigen angeregten Zuständen, *Angew. Chem.*, 2017, **129**, 5770–5776.

16 F. E. Hahn, Koordinationschemie mehrzähniger Isocyanid–Liganden, *Angew. Chem.*, 1993, **105**, 681–696.
17 F. E. Hahn, The Coordination Chemistry of Multidentate Isocyanide Ligands, *Angew. Chem., Int. Ed. Engl.*, 1993, **32**, 650–665.
18 H. V. Huynh, Y. Han, R. Jothibasu and J. an Yang, ^{13}C NMR Spectroscopic Determination of Ligand Donor Strengths Using N-Heterocyclic Carbene Complexes of Palladium(II), *Organometallics*, 2009, **28**, 5395–5404.
19 N. M. Kostic and R. F. Fenske, Molecular orbital study of bonding, conformations, and reactivity of transition-metal complexes containing unsaturated organic ligands. Electrophilic and nucleophilic additions to acetylide, vinylidene, vinyl, and carbene ligands, *Organometallics*, 1982, **1**, 974–982.
20 A. E. Carpenter, C. C. Mokhtarzadeh, D. S. Ripatti, I. Havrylyuk, R. Kamezawa, C. E. Moore, A. L. Rheingold and J. S. Figueroa, Comparative measure of the electronic influence of highly substituted aryl isocyanides, *Inorg. Chem.*, 2015, **54**, 2936–2944.
21 S. Z. Goldberg, E. N. Duesler and K. N. Raymond, Crystal and molecular structure of $[Mn(CO)_4(C_2PPh_3)Br]$—a co-ordination compound of the unusual carbonyl-ylide product, Ph_3P^+-C≡C:$^-$, *J. Chem. Soc. D*, 1971, 826–827.
22 D. K. Mitchell, W. D. Korte and W. C. Kaska, Bromotetracarbonyltriphenylphosphoranylideneketenmanganese(I): an organometallic ylide, *J. Chem. Soc. D*, 1970, 1384.
23 S. Z. Goldberg, E. N. Duesler and K. N. Raymond, Crystal and molecular structure of $[Mn(CO)_4(C_2P(C_6H_5)_3)Br]$. Coordination compound of the unusual carbonyl-ylide reaction product $(C_6H_5)_3P^+$-C≡C:$^-$, *Inorg. Chem.*, 1972, **11**, 1397–1401.
24 W. C. Kaska, D. K. Mitchell and R. F. Reichelderfer, Transition metal complexes of hexaphenylcarbodiphosphorane, *J. Organomet. Chem.*, 1973, **47**, 391–402.
25 W. C. Kaska, D. K. Mitchell, R. F. Reichelderfer and W. D. Korte, The interaction of phosphorus ylides with transition metal carbonyl compounds. Triphenylphosphinemethylene and bis(triphenylphosphine)carbon. Comparative chemistry, *J. Am. Chem. Soc.*, 1974, **96**, 2847–2854.
26 H. Blau, K.-H. Griessmann and W. Malisch, Zur reaktion von metall-koordiniertem kohlenmonoxid mit yliden, *J. Organomet. Chem.*, 1984, **263**, c5–c9.
27 W. Petz and F. Weller, Reaktion von $Ph_3P{=}C{=}PPh_3$ mit $Fe(CO)_5$; Molekülstrukturen von $(CO)_4Fe{=}C{=}C{=}PPh_3$ und $Fe_3(CO)_9(\mu^3\text{-}\eta^2\text{-}C{\equiv}C\text{-}PPh_3)$/Reaction of $Ph_3P{=}C{=}PPh_3$ with $Fe(CO)_5$; Molecular Structures of $(CO)_4Fe{=}C{=}C{=}PPh_3$ and $Fe_3(CO)_9(\mu^3\text{-}\eta^2\text{-}C{\equiv}C\text{-}PPh_3)$, *Z. Naturforsch.*, 1996, **51 b**, 1598–1604.
28 R. E. Cramer, K. T. Higa and J. W. Gilje, Uranium-carbon multiple-bond chemistry. 5. Carbon-oxygen bond cleavage in uranium phosphonium enolate manganese complex, *Organometallics*, 1985, **4**, 1140–1141.
29 F. Rosche, G. Heckmann, E. Fluck and F. Weller, Ein (Phosphonioalkinyl)- und ein Acetyl(tetracarbonyl)eisen, *Z. anorg. allg. Chem.*, 1996, **622**, 974–980.
30 K. Sünkel, Komplexchemie perhalogenierter cyclopentadiene und alkine, *J. Organomet. Chem.*, 1992, **436**, 101–108.
31 K. Sünkel and U. Birk, Coordination chemistry of perhalogenated cyclopentadienes and alkynes, XXIII: The reaction of dichloroethyne with Ni(0) phosphine complexes: the strong influences of phosphine, solvent and concentration on the product composition. Structures of Ni(PPh3)2(Cl)(C≡CCl) and [Ni(PBu3)2(C≡C-(PBu3)2]2+[SbF6−]2, *Polyhedron*, 1999, **18**, 3187–3197.
32 H. J. Bestmann, H. Behl and M. Bremer, Phosphonioboratoacetylenes: C_2 Stabilized by Donor and Acceptor Molecules, *Angew. Chem., Int. Ed. Engl.*, 1989, **28**, 1219–1221.
33 H. J. Bestmann, H. Behl and M. Bremer, Phosphonioboratoacetylene, durch Donor- und Acceptormoleküle stabilisiertes C_2, *Angew. Chem.*, 1989, **101**, 1303–1304.
34 L. Dahlenburg, A. Weiβ, M. Bock and A. Zahl, Ethinyl- und Butadiinylkomplexe des Eisens und Rutheniums mitterminalen Hauptgruppenelement-Substituenten, Cp*Fe(Ph2PCH(X)CH2PPh2)C≡CY (X = H, PPh2; Y = H, PPh2, P(+)Ph2Me) und Ru(Ph2PCH2PPh2)2(X) C≡CC≡CSiMe3 (X = Cl, C≡CC≡CSiMe3), *J. Organomet. Chem.*, 1997, **541**, 465–471.
35 L. Dahlenburg, A. Weiβ and M. Moll, Ethinylkomplexe des Rutheniums mit terminalen Hauptgruppenelement-Substituenten: Systematischer Aufbau metallgebundener Phosphoniumacetylid-Liganden R′R2P(+)-C≡C|(−), *J. Organomet. Chem.*, 1997, **535**, 195–200.
36 W. Petz, B. Neumüller and R. Tonner, Reaction of Double Ylide $C(PPh_3)_2$ with $[W(CO)_6]$ – Crystal Structures of $[(CO)_5W(CCPPh_3)]$ and $[(CO)_5W\{\eta^1\text{–}O_2C_2(PPh_3)_2\}]$ and Bonding Analyses of $[TM(CCPR_3)]$ Compounds, *Eur. J. Org. Chem.*, 2010, 1872–1880.
37 H. J. Bestmann, W. Frank, C. Moll, A. Pohlschmidt, T. Clark and A. Göller, Triphenylphosphonioacetylide: A Species Isoelectronic with Isocyanides, *Angew. Chem., Int. Ed.*, 1998, **37**, 338–342.
38 H. J. Bestmann, W. Frank, C. Moll, A. Pohlschmidt, T. Clark and A. Göller, Triphenylphosphonioacetylid: eine mit Isocyaniden isovalenzelektronische Spezies, *Angew. Chem.*, 1998, **110**, 347–351.
39 R. L. Cordiner, A. F. Hill and J. Wagler, Reactions of $[Ru(CO)_2(PPh_3)_3]$ with Alkynylphosphonium Salts: Phosphaallenylidene vs Phosphonioacetylide Coordination, *Organometallics*, 2009, **28**, 4880–4885.
40 T.-F. Leung, D. Jiang, M.-C. Wu, D. Xiao, W.-M. Ching, G. P. A. Yap, T. Yang, L. Zhao, T.-G. Ong and G. Frenking, Isolable dicarbon stabilized by a single phosphine ligand, *Nat. Chem.*, 2021, **13**, 89–93.
41 M. A. Wünsche, P. Mehlmann, T. Witteler, F. Buß, P. Rathmann and F. Dielmann, Imidazolin-2-ylidenaminophosphines as Highly Electron-Rich Ligands for

Transition-Metal Catalysts, *Angew. Chem., Int. Ed.*, 2015, **54**, 11857–11860.

42 M. A. Wünsche, P. Mehlmann, T. Witteler, F. Buß, P. Rathmann and F. Dielmann, Imidazolin-2-ylidenamino-phosphane als sehr elektronenreiche Liganden für Übergangsmetallkatalysatoren, *Angew. Chem.*, 2015, **127**, 12024–12027.

43 P. Mehlmann, C. Mück-Lichtenfeld, T. T. Y. Tan and F. Dielmann, Tris(imidazolin-2-ylidenamino)phosphine: A Crystalline Phosphorus(III) Superbase That Splits Carbon Dioxide, *Chem. – Eur. J.*, 2017, **23**, 5929–5933.

44 P. Rotering, L. F. B. Wilm, J. A. Werra and F. Dielmann, Pyridinylidenaminophosphines: Facile Access to Highly Electron-Rich Phosphines, *Chem. – Eur. J.*, 2020, **26**, 406–411.

45 F. Buß, M. Das, D. Janssen-Müller, A. Sietmann, A. Das, L. F. B. Wilm, M. Freitag, M. Seidl, F. Glorius and F. Dielmann, Photoswitchable electron-rich phosphines: using light to modulate the electron-donating ability of phosphines, *Chem. Commun.*, 2023, **59**, 12019–12022.

46 J. H. Franzen, L. F. B. Wilm, P. Rotering, K. Wurst, M. Seidl and F. Dielmann, Electron-rich pyridines with para-N-heterocyclic imine substituents: ligand properties and coordination to CO_2, SO_2, BCl_3 and Pd^{II} complexes, *Dalton Trans.*, 2024, **53**, 11876–11883.

47 J. H. Franzen, X. Zhou, K. Biv, A. Ajò, A. Mencke, L. F. B. Wilm, M. Seidl, T. S. Hofer, L. de Cola, P. Brüggeller, M. E. Thompson and F. Dielmann, Electron-rich phenanthroline bearing N-heterocyclic imine substituents: synthesis, optical properties, metal coordination, *Inorg. Chem. Front.*, 2025, DOI: **10.1039/D5QI00957J**.

48 M. Abdinejad, L. F. B. Wilm, F. Dielmann and H. B. Kraatz, Electroreduction of CO_2 Catalyzed by Nickel Imidazolin-2-ylidenamino-Porphyrins in Both Heterogeneous and Homogeneous Molecular Systems, *ACS Sustainable Chem. Eng.*, 2021, **9**, 521–530.

49 N. Kuhn, M. Göhner, M. Grathwohl, J. Wiethoff, G. Frenking and Y. Chen, 2–Iminoimidazoline—starke Stickstoffbasen als Koordinationspartner in der Anorganischen Chemie, *Z. Anorg. Allg. Chem.*, 2003, **629**, 793–802.

50 T. Ochiai, D. Franz and S. Inoue, Applications of N-heterocyclic imines in main group chemistry, *Chem. Soc. Rev.*, 2016, **45**, 6327–6344.

51 X. Wu and M. Tamm, Transition metal complexes supported by highly basic imidazolin-2-iminato and imidazolin-2-imine N-donor ligands, *Coord. Chem. Rev.*, 2014, **260**, 116–138.

52 M. Zhong and M. Yuan, Recent advances in the use of N-heterocyclic carbene adducts of N, P, C elements as supporting ligands in organometallic chemistry, *RSC Adv.*, 2025, **15**, 15052–15085.

53 P. Löwe and F. Dielmann, Crystalline phosphino(silyl)carbenes that readily form transition metal complexes, *Chem. Commun.*, 2022, **58**, 11831–11834.

54 P. Löwe, M. A. Wünsche, F. R. S. Purtscher, J. Gamper, T. S. Hofer, L. F. B. Wilm, M. B. Röthel and F. Dielmann, Terminal methylene phosphonium ions: precursors for transient monosubstituted phosphinocarbenes, *Chem. Sci.*, 2023, **14**, 7928–7935.

55 L. C. Torres, P. Löwe, A. Bhattacharjee, M. B. Röthel, M. Seidl, J. LeBlanc, K. Wurst, F. Dielmann and C. B. Caputo, Allenylidene Phosphonium Ion: An Isoelectronic Phosphorus Analogue of 3Cumulene, *Angew. Chem., Int. Ed.*, 2025, **64**, e202502201.

56 L. C. Torres, P. Löwe, A. Bhattacharjee, M. B. Röthel, M. Seidl, J. LeBlanc, K. Wurst, F. Dielmann and C. B. Caputo, Allenylidenphosphonium–Ion: Ein Isoelektronisches Phosphor–Analogon Von [3]Kumulen, *Angew. Chem.*, 2025, **137**, e202502201, DOI: **10.1002/ange.202502201**.

57 M. D. Böhme, T. Eder, M. B. Röthel, P. D. Dutschke, L. F. B. Wilm, F. E. Hahn and F. Dielmann, Synthese N – heterocyclischer Carbene und ihrer Komplexe durch Chloroniumionabstraktion von 2–Chlorazoliumsalzen mit elektronenreichen Phosphanen, *Angew. Chem.*, 2022, **134**, e202202190, DOI: **10.1002/ange.202202190**.

58 M. D. Böhme, T. Eder, M. B. Röthel, P. D. Dutschke, L. F. B. Wilm, F. E. Hahn and F. Dielmann, Synthesis of N-Heterocyclic Carbenes and Their Complexes by Chloronium Ion Abstraction from 2-Chloroazolium Salts Using Electron-Rich Phosphines, *Angew. Chem., Int. Ed.*, 2022, **61**, e202202190.

59 F. Buß, M. B. Röthel, J. A. Werra, P. Rotering, L. F. B. Wilm, C. G. Daniliuc, P. Löwe and F. Dielmann, Tris(tetramethylguanidinyl)phosphine: The simplest non-ionic phosphorus superbase and strongly-donating phosphine ligand, *Chem. – Eur. J.*, 2022, **28**, e202104021, DOI: **10.1002/chem.202104021**.

60 M. Asay, B. Donnadieu, W. W. Schoeller and G. Bertrand, Synthesis of allenylidene lithium and silver complexes, and subsequent transmetalation reactions, *Angew. Chem., Int. Ed.*, 2009, **48**, 4796–4799.

61 V. Lavallo, Y. Ishida, B. Donnadieu and G. Bertrand, Isolation of Cyclopropenylidene–Lithium Adducts: The Weiss–Yoshida Reagent, *Angew. Chem.*, 2006, **118**, 6804–6807.

62 C. E. Mortimer and U. Müller, *Chemie*, Georg Thieme Verlag, Stuttgart, New York, 13th edn, 2020.

63 A. F. Hollemann, E. Wiberg and N. Wiberg, *Anorganische Chemie Band 1: Grundlagen und Hauptgruppenelemente*, de Gruyter, Berlin, 103rd edn, 2017.

64 P. Groth, H. Møllendal, R. Seip, J. Weidlein and K. Spahiu, On the Crystal Structure of the (1 : 1) Complex between Lithium Thiocyanate and 1,4,7,10-Tetraoxacyclododecane at Room Temperature, *Acta Chem. Scand., Ser. A*, 1981, **35**, 463–465.

65 F. Pauer, J. Rocha and D. Stalke, Synthesis and crystal structure of bis(12-crown-4)lithium bis[N,N′-bis(trimethylsilyl) benzenesulphinamidino]lithiate(1−-); the first observation of three different lithium-7 environments in high-resolution solid-state NMR spectroscopy, *J. Chem. Soc., Chem. Commun.*, 1991, 1477–1479.

66 O. Grounds, M. Zeller and S. V. Rosokha, Structural preferences in strong anion–π and halogen-bonded complexes: π- and σ-holes vs. frontier orbitals interaction, *New J. Chem.*, 2018, **42**, 10572–10583.
67 K. Bläsing, J. Bresien, S. Maurer, A. Schulz and A. Villinger, Trimethylsilyl Pseudohalide Adducts of $GaCl_3$ and $B(C_6F_5)_3$, *Chem. Ber.*, 2021, **2021**, 1913–1920.
68 X. Zhao, A. J. Lough and D. W. Stephan, Synthesis and reactivity of alkynyl-linked phosphonium borates, *Chem. – Eur. J.*, 2011, **17**, 6731–6743.
69 K. Škoch, C. G. Daniliuc, M. Müller, S. Grimme, G. Kehr and G. Erker, Stereochemical Behavior of Pairs of P-stereogenic Phosphanyl Groups at the Dimethylxanthene Backbone, *Chem. – Eur. J.*, 2022, **28**, e202200248.
70 E. D. Amoateng, J. Zamora-Moreno, G. Kuchenbeiser, B. Donnadieu, F. Tham, V. Montiel-Palma and T. K. Hollis, Investigating intermediates in the CCC–NHC pincer ligand metalation/transmetalation to Rh sequence, an improved stoichiometric synthesis of CCC–NHC pincer Rh complexes, *J. Organomet. Chem.*, 2022, **979**, 122499.
71 L. J. Watson and A. F. Hill, A Metallabicycle From Thiocarbonyl-Cyclopropenium Coupling, *Chem. – Eur. J.*, 2023, **29**, e202301753.
72 C. A. Tolman, Steric effects of phosphorus ligands in organometallic chemistry and homogeneous catalysis, *Chem. Rev.*, 1977, **77**, 313–348.
73 M.-C. Wu, Y.-F. Liang, T. Jurca, G. P. A. Yap, T.-F. Leung and T.-G. Ong, Reactive Dicarbon as a Flexible Ligand for Transition-Metal Coordination and Catalysis, *J. Am. Chem. Soc.*, 2022, **144**, 12996–13005.
74 D. G. Gusev, Electronic and Steric Parameters of 76 N-Heterocyclic Carbenes in $Ni(CO)_3$ (NHC), *Organometallics*, 2009, **28**, 6458–6461.
75 H. V. Huynh, Electronic Properties of N-Heterocyclic Carbenes and Their Experimental Determination, *Chem. Rev.*, 2018, **118**, 9457–9492.
76 R. Dorta, E. D. Stevens, N. M. Scott, C. Costabile, L. Cavallo, C. D. Hoff and S. P. Nolan, Steric and electronic properties of N-heterocyclic carbenes (NHC): a detailed study on their interaction with $Ni(CO)_4$, *J. Am. Chem. Soc.*, 2005, **127**, 2485–2495.
77 C. A. Tolman, Electron donor-acceptor properties of phosphorus ligands. Substituent additivity, *J. Am. Chem. Soc.*, 1970, **92**, 2953–2956.
78 L. Falivene, Z. Cao, A. Petta, L. Serra, A. Poater, R. Oliva, V. Scarano and L. Cavallo, Towards the online computer-aided design of catalytic pockets, *Nat. Chem.*, 2019, **11**, 872–879.
79 A. Poater, F. Ragone, S. Giudice, C. Costabile, R. Dorta, S. P. Nolan and L. Cavallo, Thermodynamics of N-Heterocyclic Carbene Dimerization: The Balance of Sterics and Electronics, *Organometallics*, 2008, **27**, 2679–2681.
80 A. Poater, F. Ragone, R. Mariz, R. Dorta and L. Cavallo, Comparing the enantioselective power of steric and electrostatic effects in transition-metal-catalyzed asymmetric synthesis, *Chem. – Eur. J.*, 2010, **16**, 14348–14353.
81 D. Holschumacher, T. Bannenberg, C. G. Hrib, P. G. Jones and M. Tamm, Heterolytic dihydrogen activation by a frustrated carbene-borane Lewis pair, *Angew. Chem., Int. Ed.*, 2008, **47**, 7428–7432.
82 P. A. Chase and D. W. Stephan, Hydrogen and amine activation by a frustrated Lewis pair of a bulky N-heterocyclic carbene and $B(C_6F_5)_3$, *Angew. Chem., Int. Ed.*, 2008, **47**, 7433–7437.
83 G. C. Welch and D. W. Stephan, Facile heterolytic cleavage of dihydrogen by phosphines and boranes, *J. Am. Chem. Soc.*, 2007, **129**, 1880–1881.
84 (*a*) P. Löwe, CCDC 2456627: Experimental Crystal Structure Determination, 2025, DOI: **10.5517/ccdc.csd.cc2ngb1j**; (*b*) K. Wurst, CCDC 2456628: Experimental Crystal Structure Determination, 2025 DOI: **10.5517/ccdc.csd.cc2ngb2k**; (*c*) K. Wurst, CCDC 2456629: Experimental Crystal Structure Determination, 2025, DOI: **10.5517/ccdc.csd.cc2ngb3l**; (*d*) K. Wurst, CCDC 2456630: Experimental Crystal Structure Determination, 2025, DOI: **10.5517/ccdc.csd.cc2ngb4m**; (*e*) K. Wurst, CCDC 2456631: Experimental Crystal Structure Determination, 2025, DOI: **10.5517/ccdc.csd.cc2ngb5n**; (*f*) A. Pöthig and S. Hohloch, CCDC 2456632: Experimental Crystal Structure Determination, 2025, DOI: **10.5517/ccdc.csd.cc2ngb6p**; (*g*) K. Wurst, CCDC 2456633: Experimental Crystal Structure Determination, 2025, DOI: **10.5517/ccdc.csd.cc2ngb7q**; (*h*) K. Wurst, CCDC 2456634: Experimental Crystal Structure Determination, 2025, DOI: **10.5517/ccdc.csd.cc2ngb8r**; (*i*) M. Seidl, CCDC 2472604: Experimental Crystal Structure Determination, 2025, DOI: **10.5517/ccdc.csd.cc2nzyf1**.